

## Collective effects on the settling of clay flocs

Ali, W.; Kirichek, A.; Chassagne, C.

**DOI**

[10.1016/j.clay.2024.107399](https://doi.org/10.1016/j.clay.2024.107399)

**Publication date**

2024

**Document Version**

Final published version

**Published in**

Applied Clay Science

**Citation (APA)**

Ali, W., Kirichek, A., & Chassagne, C. (2024). Collective effects on the settling of clay flocs. *Applied Clay Science*, 254, Article 107399. <https://doi.org/10.1016/j.clay.2024.107399>

**Important note**

To cite this publication, please use the final published version (if applicable).  
Please check the document version above.

**Copyright**

Other than for strictly personal use, it is not permitted to download, forward or distribute the text or part of it, without the consent of the author(s) and/or copyright holder(s), unless the work is under an open content license such as Creative Commons.

**Takedown policy**

Please contact us and provide details if you believe this document breaches copyrights.  
We will remove access to the work immediately and investigate your claim.



## Technical Note

## Collective effects on the settling of clay flocs

W. Ali<sup>a,\*</sup>, A. Kirichek<sup>b</sup>, C. Chassagne<sup>a</sup><sup>a</sup> Section of Environmental Fluid Mechanics, Department of Hydraulic Engineering, Faculty of Civil Engineering and Geosciences, Delft University of Technology, Stevinweg 1, 2628 CN Delft, the Netherlands<sup>b</sup> Section of Rivers, Ports, Waterways and Dredging Engineering, Department of Hydraulic Engineering, Faculty of Civil Engineering and Geosciences, Delft University of Technology, Stevinweg 1, 2628 CN Delft, the Netherlands

## ARTICLE INFO

## Keywords:

Flocculation  
Settling velocities  
Organic matter  
Cohesive sediment

## ABSTRACT

In this work a high-magnification digital video camera in combination with a settling column is used to study in a first part the influence of the amount of flocs transferred into the settling column on their settling velocity. In a second part, the setup was used to study the properties of flocs prepared at different clay concentrations but at same flocculant to clay ratio (2.5 mg g<sup>-1</sup>). Illite clay was used and flocculated in a 1 L jar with an anionic polyacrylamide (flocculant). Results show that the average settling velocity of flocs is a function of the amount of transferred flocs. It was also found that floc size and settling velocity depend on clay concentration. This is attributed to the fast aggregation happening in the jar when flocculant and clay are mixed: at higher clay concentrations, larger flocs are created in the first minutes of the experiment, with low densities that prevent them from settling to the bottom of the jar.

## 1. Introduction

Estuarine mud particles can flocculate and form aggregates called “flocs”. The sediment having the ability to flocculate is usually referred to as “cohesive sediment” (Whitehouse et al., 2000; Mehta, 2014; Chassagne, 2020). Cohesive sediment can adsorb contaminants and nutrients, which has a direct impact on water quality and biota (Uncles et al., 1998). Flocs are formed in response to a change in environmental conditions (hydrodynamics, salinity, presence of organic matter...), which occurs principally in estuarine regions. As these regions are of great importance for human activities, an ongoing research topic is to refine sediment transport models such as to incorporate cohesive sediment transport (Geyer et al., 2000; Cheviet et al., 2002; Ali and Chassagne, 2022).

Flocs are composed of mineral clay bound to organic matter particles with entrapped water. Organic matter and salinity strongly influence the cohesiveness and flocculation ability of sediment, and hereby its deposition, consolidation, and erodibility (Nowell et al., 1981; Heinzelmann and Wallisch, 1991; Safar, 2022; Van Leussen, 1999). There is very large spread in settling velocity (and hence in density) for flocs in the range of 50–150 μm (Khelifa and Hill, 2006; Maggi, 2013; Safar, 2022). It is usually found that flocs' density is a decreasing function of their size (McDowell and O'Connor, 1977; Dyer and Manning, 1999; Klimpel and

Hogg, 1986; Droppo et al., 2000; Khelifa and Hill, 2006).

For long-time particle size measurements, in situ laser-based diffraction techniques are used, such as the Sequoia Scientific Laser In-situ Scattering and Transmissometry (LISST) 100× and 200×, that measure floc size and volume concentration (Agrawal and Pottsmith, 2000). From this data, the density of flocs and settling fluxes can be estimated based on Stokes' law. It was shown that when flocs are heterogeneous in composition and have a non-spherical structure, the results obtained from LISST are subject to caution (Mikkelsen et al., 2005; Smith and Friedrichs, 2011). Furthermore, in salinity-driven pycnoclines where the Schlieren effect influences measured sizes, LISSTs may provide ambiguous data (Karageorgis et al., 2015; Chapalain et al., 2019). For these reasons, additional monitoring campaigns are usually planned episodically during the long-time measurement series, to sample flocs from the water column and assess their properties using video microscopy-based techniques (Law et al., 1997; Manning et al., 2011; Manning, 2015; Fall et al., 2021). These techniques involve transferring a few mL of the collected sample into a settling column and record the settling of the transferred particles. These particles at first form a small cloud, that breaks up as particles start to settle.

It is known from studying the physics of the settling of a cloud of particles in quiescent water that the settling velocity of the cloud is proportional to the number of particles inside the cloud (Guazzelli and

\* Corresponding author.

E-mail address: [w.ali@tudelft.nl](mailto:w.ali@tudelft.nl) (W. Ali).<https://doi.org/10.1016/j.clay.2024.107399>

Received 17 November 2023; Received in revised form 27 April 2024; Accepted 29 April 2024

Available online 3 May 2024

0169-1317/© 2024 The Authors. Published by Elsevier B.V. This is an open access article under the CC BY license (<http://creativecommons.org/licenses/by/4.0/>).

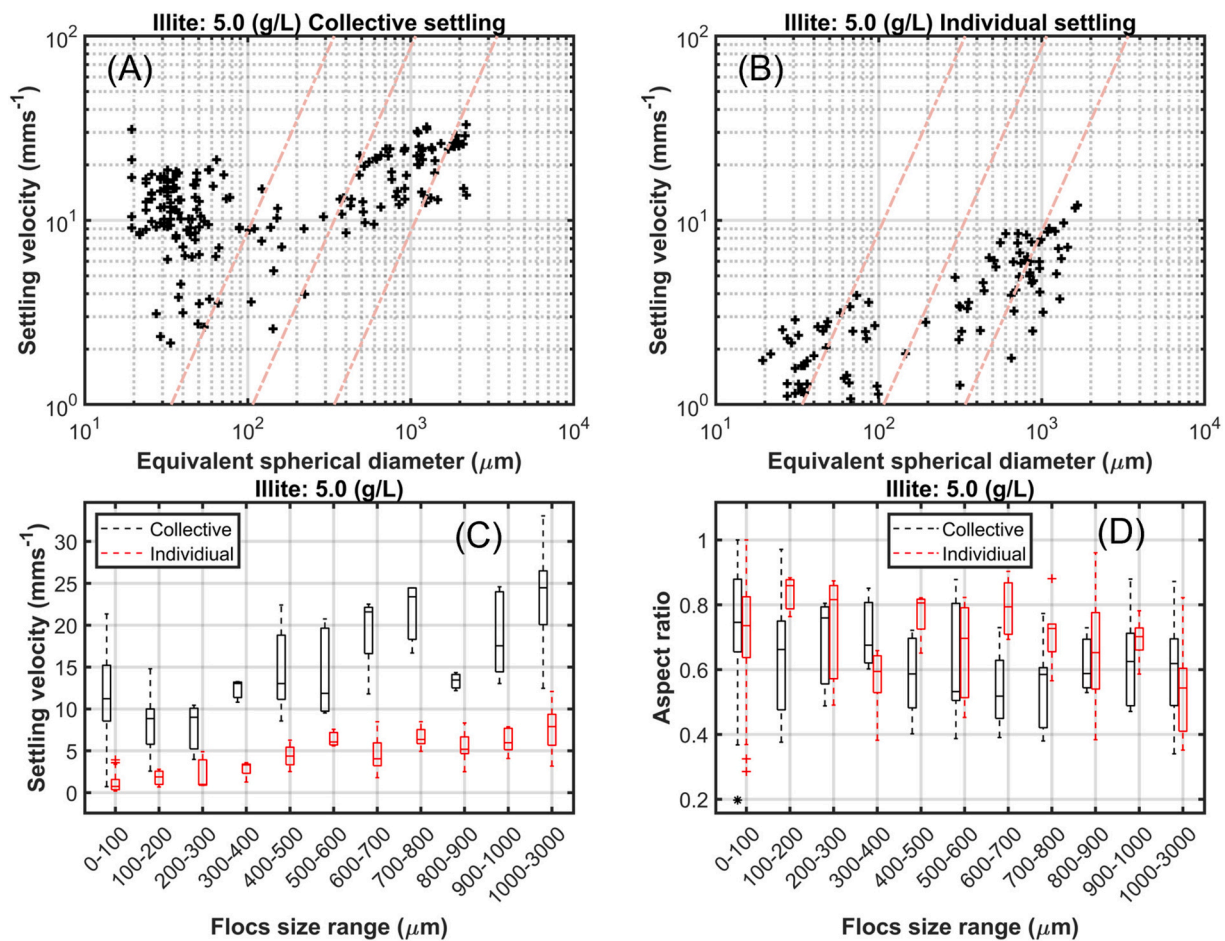


**Fig. 1.** Settling velocity and particle size analysis of  $5 \text{ g L}^{-1}$  experiment for both collective (A) and individual settling (B) cases. Settling velocity is plotted as a function of equivalent spherical diameter, with diagonal dashed lines representing effective density isolines calculated by using Stokes equation (from left to right:  $1600, 160, 16 \text{ (kg m}^{-3}\text{)}$ ). Fig. (C), shows settling velocity comparison in both cases, whereas Fig. (D) shows the comparison between aspect ratio.

Morris, 2011). Consequently, the settling velocity of a particle in a cloud can be orders of magnitude larger than the Stokes velocity of the same isolated particle. In the experiments, the measurements are performed at the bottom of the settling column after the cloud has broken up, and where particles are expected to settle according to Stokes. The density of flocs can then be estimated from particle size and settling velocity. The first objective of the work presented in this article is to measure the settling velocities as a function of the amount of transferred flocs and check whether these velocities are (or not) dependent on the amount of transferred flocs. A second objective is to study the dependence of flocs settling velocities and sizes for samples made at different clay concentrations, at the same flocculant to clay ratio to test the hypothesis that floc sizes should be a function of flocculant to clay ratio only.

## 2. Material and methods

The illite clay (100% illite) used in the experiments was obtained as a dry powder from Argiletz laboratories. This clay was selected as being of interest for our study on turbidity currents (Ali et al., 2022). The illite particle's  $D_{50}$  was determined to be approximately  $5 \mu\text{m}$  using Malvern Master Sizer 2000, a technique that relies on static light scattering for measurement (see Fig. S1 supplementary material online).

Zetag 4110, an anionic polyacrylamide (produced by BTC Europe GmbH) with a medium anionic charge and a high molecular weight, was used as a flocculant in this study.  $2.5 \text{ mg g}^{-1}$  flocculant to clay ratio was used for flocculation, which is close to the optimum dosage for this flocculant (Shakeel et al., 2020). Eight different clay concentrations

( $0.01, 0.025, 0.1, 0.5, 1.0, 1.5, 2.0$  and  $5.0 \text{ g L}^{-1}$ ) were used and flocculated by addition of flocculant, keeping the ratio of clay concentration to flocculant concentration constant. All suspensions were flocculated by stirring them using a rectangular impeller in a 1 L jar (see Fig. S2) for 1 h at  $50 \text{ s}^{-1}$ , which was enough to reach equilibrium floc size. It was observed that for the samples with clay concentration below  $0.1 \text{ g L}^{-1}$ , the created flocs settled at the bottom of their respective jars within 5 min. The action of the impeller (located 5 cm above the bottom of the jar) then only mobilized them at the bottom of the jar for the remaining of the hour. For the samples with clay concentration above  $0.1 \text{ g L}^{-1}$ , the flocs were formed very rapidly and remained in suspension for the whole hour. After one hour of stirring, the stirrer was stopped, flocs settled and were sampled at the bottom of the jar.

All suspensions were made using tap water. The composition of tap water provided by the drinking water company Evides is shown in Table S0 for the days the experiments were conducted.

### 2.1. Floc size and settling analysis

#### 2.1.1. FLOCCAM

The FLOCCAM setup (see Fig. S3) comprises a rectangular settling column and employs video microscopy to assess particle size distributions (PSDs) for particles larger than  $20 \mu\text{m}$  and their settling velocities. The settling column measures  $10 \text{ cm} \times 10 \text{ cm} \times 30 \text{ cm}$  and features glass panels on the front and rear, along with plastic sides. The camera used is a 5MP CMOS camera with a resolution of  $2592 \times 2048$  pixels, a  $4.8 \mu\text{m}$  pixel size, and a Global Shutter, known as iDS UI-3180CP-M-GL Rev.2.1

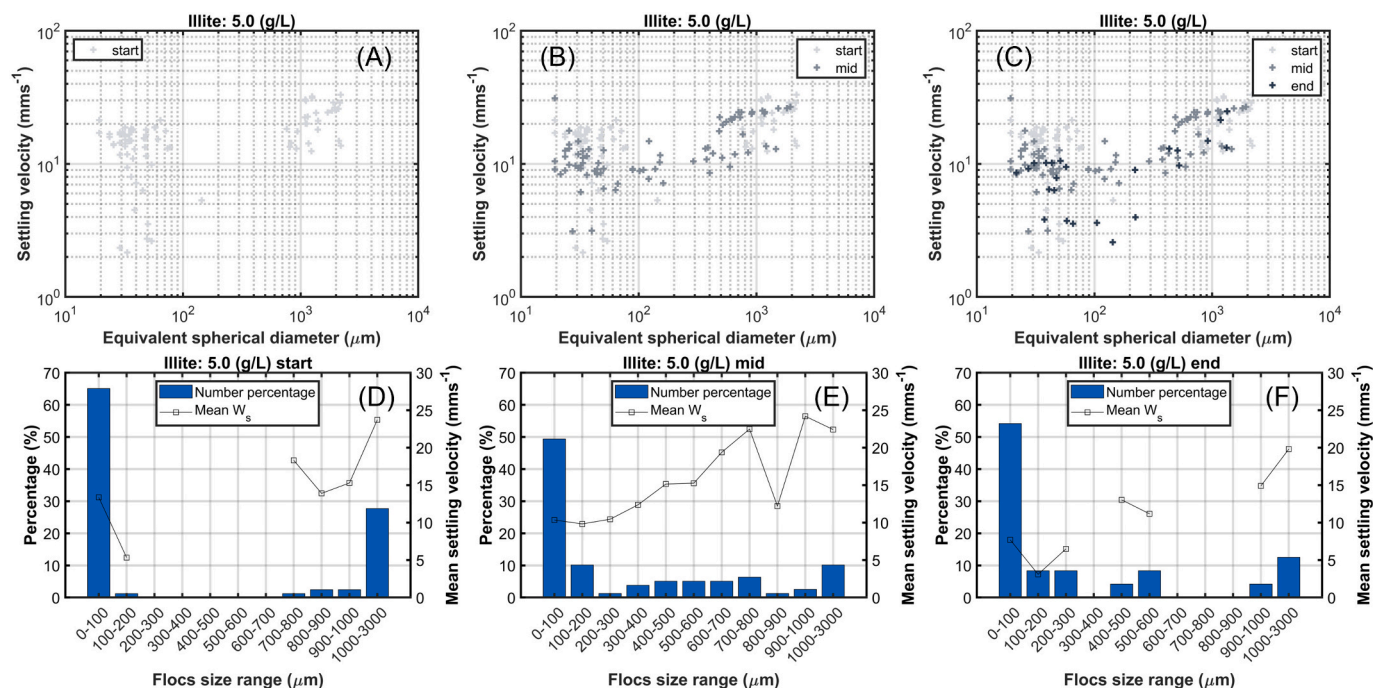


Fig. 2. Figs. (A,B,C) Settling velocity and particle size analysis of 5 g L<sup>-1</sup> experiment at three different times, e.g. start, middle and end. Figs. (D,E,F) show floc size bin range and mean settling velocity corresponding to Figs. (A,B,C) respectively.

(AB02546). This camera is paired with the S5VPJ2898 telecentric lens which offers an adjustable working distance and a C-mount, manufactured by Sill Optics GmbH & Co. KG. The flocs were collected using a pipette with an aperture of 5 mm, which is large enough to minimize the breaking of the collected flocs. The aperture of the pipette was brought into contact with the water surface, allowing the flocs to settle under their weight into the settling column. In the experiments, a volume of roughly 2 mL was transferred from the pipette into the 3 L settling column, filled with the same tap water as the jars. The flocs were then recorded 10 cm above the bottom of the settling column while they were settling, and their size, shape and settling velocity were determined. The set-up used in our experiments makes use of the natural breakup of a particle cloud upon settling. When the flocs are recorded by the camera, it is expected that each floc has reached its Stokes settling velocity and, hence, is not influenced by the presence of neighbouring flocs. Analysis of recorded settling floc videos in the settling column, including PSD, size, aspect ratio, and settling velocity calculations, was performed using the Safas software package (MacIver, 2019). The size of flocs was estimated using the relation  $R = \sqrt{a \times b}$ , where  $a$  is the major and  $b$  the minor axis of the particle.

### 3. Results and discussion

#### 3.1. Individual vs collective settling

The results of 5.0 g L<sup>-1</sup> illite flocculated with 2.5 mg g<sup>-1</sup> flocculant to clay ratio are shown in Fig. 1. Two cases (“collective and individual settling”) are displayed. “Collective settling” refers to experiments whereby a subsample with a substantial amount of flocs was collected at the bottom of the jar and transferred into the settling column, as is usually done when performing this type of measurements (Manning et al., 2010). The combined results of three such samplings are presented in the graphs (Fig. 1 (B)). “Individual settling” refers to experiments whereby one floc at the time was sampled at the bottom of the jar and transferred to the settling column.

It is found that in the case of collective settling, the settling velocity is much higher than for individual settling for all size classes. For

individual settling, it is observed that the settling velocity is increasing with floc size, as expected. For collective settling, broad ranges of settling velocities are found for each class of particle sizes. From the video recording, it could be observed that, indeed, flocs settling in the same frames had the same settling velocity, irrespective of their size.

From video analysis, it was also found that the mean aspect ratio of flocs in both individual and collective settling cases is 0.7 (see Fig. 1(D)), indicating that the flocs are not quite spherical. In both cases (and especially in the collective settling case), some flocs were observed to be obtained from differential settling in the column (see Fig. S4). In Fig. 2, the scatter plot of the settling velocity vs equivalent spherical floc size for the collective settling case at three different times during the settling are shown, labelled “start” (first flocs to be recorded), “mid” (flocs recorded after the first flocs), and “end” (last flocs to be recorded). Snapshots taken during these different times are displayed in Fig. S4. From the scatter plots it was found that, as expected, particles settling fastest were observed in the start frames and particles settling slowest in the end frames. The mean settling velocity of flocs found in the size range of 20–100 μm is similar to the settling velocity of bigger flocs (>700 μm) for all times (“start”, “mid” or “end”). From these results, it can be concluded that small flocs are always entrained in the wake of the large ones, matching their velocity.

Similar results were obtained by Dyer and Manning (1999) for the settling velocity of flocs from the Tamar estuary: when only a few flocs are sampled (as in Fig. 2, top graph in Dyer and Manning (1999)) the flocs have a settling velocity that increases with floc size, following a constant effective isodensity line of 16 kg m<sup>-3</sup>. When a lot of flocs are sampled (as in Fig. 2, the bottom graph in Dyer and Manning (1999)), a large horizontal band of points, representing flocs of sizes in the range 20–500 μm are found in the range of 10 mm s<sup>-1</sup>. This implies that flocs of sizes smaller than 100 μm would have an equivalent effective density much larger than 1600 kg m<sup>-3</sup> if the Stokes settling formula is applied. Dyer and Manning (1999) attribute this very high density to the presence of crystals of hornblende and tourmaline, which indeed can have densities as high as 3400 kg m<sup>-3</sup>. However, for 50 μm particles reaching 10 mm s<sup>-1</sup> it would imply that these particles have a density of 8600 kg m<sup>-3</sup> (density of brass), which would be unlikely.

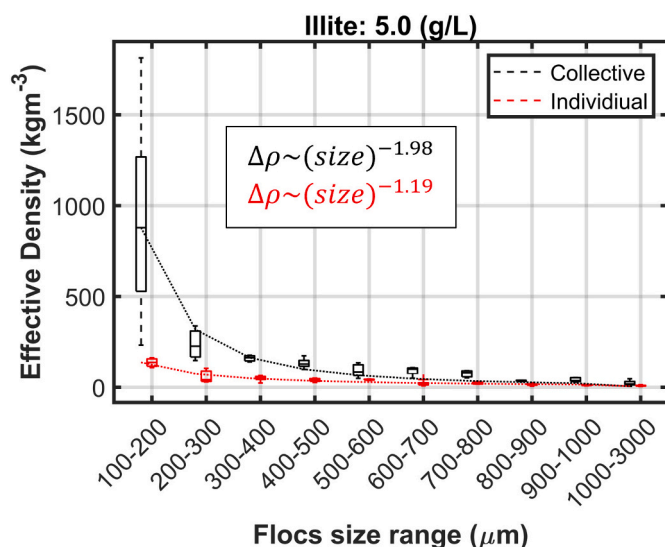


**Fig. 3.** Effective density as a function of floc size range for both collective and individual cases for 5 g L<sup>-1</sup> experiment. The fit is performed for floc sizes above 100 μm; for fits for all bin size see Fig. S5. The effective density was estimated from Stoke's Law  $\Delta\rho = \rho_{floc} - \rho_{water} = 9\eta\nu/2gR^2$  where  $\eta$  and  $\rho_{water}$  the viscosity and density of water,  $\nu$  the floc measured settling velocity,  $g$  the gravitational acceleration and  $R$  the floc size.

Using Stokes equation, the effective density of flocs (i.e. their density minus the density of water) was estimated, which is shown in Fig. 3. The decreasing effective density as function of particle size was fitted, as is often done in literature, using a negative power law of the size (Klimpel and Hogg, 1986; Droppo et al., 2000; Khelifa and Hill, 2006). The effective density was fitted by accounting or not for the first bin size of 0–100 μm, as displayed in the insert of Fig. 3 and Fig. S5. It was found that the exponent “n” varied significantly in both collective and individual settling cases and also when accounting or not for the 0–100 μm size range. The highest effective densities are found for the smallest particles (around 20 μm in size, which is the camera detection limit). This small study demonstrates that caution should be taken when discussing the value of “n” as being a material parameter for a given suspension. Often, “n” is said to be related to a fractal dimension (Winterwerp, 1998). A discussion about fractal dimension is given in Chassagne et al. (2021).

### 3.2. Clay concentration dependence

For the results presented in this section, subsamples of flocculated material were carefully collected at the bottom of the jars and transferred into the settling column (“collective settling”). The distribution in

floc size (boxplots) for the investigated clay concentrations is shown in Fig. 4(A). For concentrations up to 0.1 g L<sup>-1</sup>, it was observed that flocs formed and settled at the bottom of the jar within 5 min. This results in floc size distributions being very similar for these low concentrations. It also indicates that flocs did not further flocculate once they had settled at the bottom of the jar, despite the action of the stirrer that agitated the water for one hour: contacts between flocs at the bottom of the jar did not result in significant sticking between flocs. For concentrations larger than 0.1 g L<sup>-1</sup>, large flocs formed rapidly, resulting in flocs with a density low enough to keep them in suspension for an hour. Large floc sizes are, therefore, observed at high clay concentrations. Fig. 4(B,C) shows the settling velocity for different concentrations of clay for the floc size ranges 20–100 μm and 900–1000 μm. Larger settling velocities are found above 0.1 g L<sup>-1</sup> for particles in the 20–100 μm range, indicating these small flocs settle in the wake of the large flocs formed above 0.1 g L<sup>-1</sup>.

## 4. Conclusions

In this work, a video-based setup was used to study flocs' settling velocities. It was shown that “collective settling”, whereby particles settle in the wake of others occurs even at low amount of sampled flocs when flocs, brought into contact with water, have reached the position of 20 cm below the air/water interface. Their terminal velocities are then roughly one order of magnitude larger than flocs that were settling individually (“individual settling”). This implies that extremely low amounts of particles should be used in this type of settling column experiments to estimate realistic individual settling velocities. The use of a video image-based device to record floc sizes also enables to pinpoint the shortcomings of laser diffraction particle sizers for flocs. Flocs have a strong size-dependent density, because flocs of larger sizes contain more flocculant. Consequently, flocs have a size-dependent refractive index. Large flocs also have a complex structure. It is, therefore, not yet clear what errors are made when converting the laser diffraction data into particle sizes. The combined use of video microscopy and laser diffraction techniques will, in the future, enable to answer this question.

In a second study, the “collective settling” method was used to compare flocs properties for flocs created in a jar, at different clay concentrations but same same flocculant to clay ratio. It was found that both size and settling velocities depended on clay concentration. The reason is linked to flocculation kinetics: at large clay concentrations, (large) flocs can be formed rapidly. At lower clay concentrations, the flocculation kinetics are slower and thus, flocs settle to the bottom of the jar within 5 min after mixing clay and flocculant. This is reflected in the density of flocs: large flocs (that remain in suspension in the jar) have a very low density (their effective density is in the range 10–30 kg m<sup>-3</sup>) whereas small flocs (containing relatively more clay) have, on average, a ten times higher relative density.

This last result can be of interest to the study of in-situ flocculation.

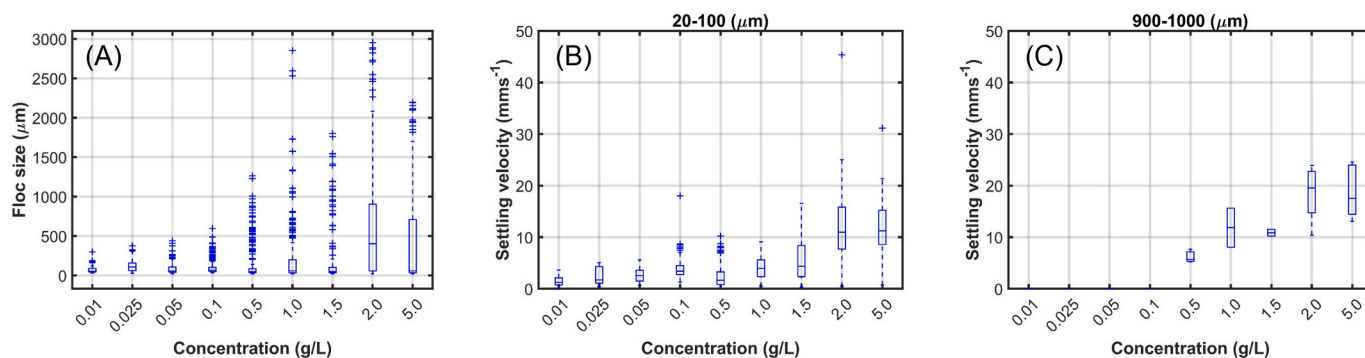


**Fig. 4.** (A): Floc size plotted for different concentrations. Fig. (B): Settling velocity of floc size range between 20 and 100 μm. Fig. (C): settling velocity of floc size range between 900 and 1000 μm. Raw data is shown in Fig. S6.

Most flocculation occurs in regions of high fine sediment concentration, such as in the water body close to the sediment bed. Not only the flocculant (organic matter) to clay ratio but also clay concentration in the water column are, therefore, factors determining both the size and density of the floc. At high clay concentrations, flocculation will occur at short timescales (minutes), and large flocs with low density will be formed that can be transported over large distances. At moderate/low clay concentration, smaller and denser flocs will be formed. Further growth of these flocs will be prevented as these flocs will rapidly settle onto the bed.

### CRedit authorship contribution statement

**W. Ali:** Writing – review & editing, Writing – original draft, Visualization, Validation, Software, Resources, Methodology, Investigation, Formal analysis. **A. Kirichek:** Writing – review & editing, Supervision, Resources, Methodology, Conceptualization. **C. Chassagne:** Writing – review & editing, Supervision, Resources, Project administration, Methodology, Funding acquisition, Conceptualization.

### Declaration of competing interest

The authors declare that they have no known competing financial interests or personal relationships that could have appeared to influence the work reported in this paper.

### Data availability

The authors confirm that the data supporting the findings of this study are available within the article and its supplementary materials. All data is fully available to all interested in the topic and upon request.

### Acknowledgement

This work is performed in the framework of PlumeFloc (TMW. BL.019.004, Topsector Water and Maritiem: Blauwe route) within the MUDNET academic network. The authors would like to thank all co-funding partners. The authors would also like to thank Deltares for using their experimental facilities in the framework of the MoU between TU Delft/Deltares.

### Appendix A. Supplementary data

Supplementary data to this article can be found online at <https://doi.org/10.1016/j.clay.2024.107399>.

### References

- Agrawal, Y.C., Pottsmith, H.C., 2000. Instruments for particle size and settling velocity observations in sediment transport. *Mar. Geol.* 168, 89–114. [https://doi.org/10.1016/S0025-3227\(00\)00044-X](https://doi.org/10.1016/S0025-3227(00)00044-X).
- Ali, W., Chassagne, C., 2022. Comparison between two analytical models to study the flocculation of mineral clay by polyelectrolytes. *Cont. Shelf Res.* 250, 104864. ISSN 0278-4343. <https://doi.org/10.1016/j.csr.2022.104864>.
- Ali, W., Enthoven, D., Kirichek, A., Helmons, R., Chassagne, C., 2022. Effect of flocculation on turbidity currents. *Front. Earth Sci.* 10, 1014170 <https://doi.org/10.3389/feart.2022.1014170>.
- Chapalain, M., Verney, R., Fettweis, M., Jacquet, M., Le Berre, D., Le Hir, P., 2019. Investigating suspended particulate matter in coastal waters using the fractal theory. *Ocean Dyn.* 69 (1), 59–81. <https://doi.org/10.1007/s10236-018-1229-6>.
- Chassagne, C., 2020. *Introduction to Colloid Science*. Delft Academic Press. ISBN 9789065624376.
- Chassagne, C., Safar, Z., Deng, Z., He, Q., Manning, A., 2021. Flocculation in estuaries: Modeling, laboratory and in-situ studies. In: *Sediment Transport-Recent Advances*. IntechOpen.
- Cheviet, C., Violeau, D., Guesmia, M., 2002. Numerical simulation of cohesive sediment transport in the Loire estuary with a three-dimensional model including new parameterisations. In: *Fine Sediment Dynamics in the Marine Environment Proc. in Mar. Sci.* 5. Elsevier, Amsterdam, pp. 529–543.
- Droppo, I.G., Walling, D., Ongley, E., 2000. The influence of floc size, density and porosity on sediment and contaminant transport. *J. Nat. Centre Scientific Res.* 4, 141–147.
- Dyer, K.R., Manning, A.J., 1999. Observation of the size, settling velocity and effective density of flocs, and their fractal dimensions. *J. Sea Res.* 41, 87–95.
- Fall, K.A., Friedrichs, C.T., Massey, G.M., Bowers, D.G., Smith, S.J., 2021. The importance of organic content to fractal floc properties in estuarine surface waters: Insights from video, LISST, and pump sampling. *J. Geophys. Res. Oceans* 126, 1–25. <https://doi.org/10.1029/2020jc016787>.
- Geyer, W.R., Hill, P.S., Milligan, T.G., Traykovski, P., 2000. The structure of the Eel River plume during floods. *Cont. Shelf Res.* 20, 2067–2093.
- Guazzelli, E., Morris, J.F., 2011. *A Physical Introduction to Suspension Dynamics*, vol. 45. Cambridge University Press.
- Heinzlmann, C.H., Wallisch, S., 1991. Benthic settlement and bed erosion. A review. *J. Hydraul. Res.* 29, 355–371.
- Karageorgis, A., Georgopoulos, D., Gardner, W., Mikkelsen, O., Velaoras, D., 2015. How Schlieren affects beam transmissometers and LISST-Deep: an example from the stratified Danube River delta, NW Black Sea. *Mediterr. Mar. Sci.* 16, 366–372. <https://doi.org/10.12681/mms.1116>.
- Khelifa, A., Hill, P.S., 2006. Models for effective density and settling velocity of flocs. *J. Hydraul. Res.* 44 (3), 390–401.
- Klimpel, R.C., Hogg, R., 1986. Effects of flocculation conditions on agglomerate structure. *J. Colloid Interface Sci.* 113 (1), 121–131.
- Law, D.J., Bale, A.J., Jones, S.E., 1997. Adaptation of focused beam reflectance measurement to in-situ particle sizing in estuaries and coastal waters. *Mar. Geol.* 140, 47–59.
- MacIver, M.R., 2019. Safas: Sedimentation and floc analysis software. <https://github.com/rmaciver/safas>.
- Maggi, F., 2013. The settling velocity of mineral, biomineral, and biological particles and aggregates in water. *J. Geophys. Res. Oceans* 118 (4), 2118–2132.
- Manning, A.J., 2015. LabSFLOC-2 – The Second Generation of the Laboratory System to Determine Spectral Characteristics of Flocculating Cohesive and Mixed Sediments. HR Wallingford Report.
- Manning, A.J., Baugh, J.V., Spearman, J.R., Whitehouse, Richard J.S., 2010. Flocculation settling characteristics of mud: sand mixtures. *Ocean Dyn.* 60, 237–253. <https://doi.org/10.1007/s10236-009-0251-0>.
- Manning, A.J., Baugh, J.V., Soulsby, R.L., Spearman, J.R., Whitehouse, R.J.S., 2011. Cohesive sediment flocculation and the application to settling flux modelling. In: Ginsberg, S.S. (Ed.), *Sediment Transport*. Rijeka, Croatia, InTech.
- McDowell, D.N., O'Connor, B.A., 1977. *Hydraulic Behaviour of Estuaries*. MacMillan, London.
- Mehta, A.J., 2014. *An Introduction to Hydraulics of Fine Sediment Transport*. Advanced Series on Ocean Engineering, 38. World Scientific Publishing Co., Hackensack, NJ.
- Mikkelsen, O.A., Hill, P.S., Milligan, T.G., Chant, R.J., 2005. In situ particle size distributions and volume concentrations from a LISST-100 laser particle sizer and a digital floc camera. *Cont. Shelf Res.* 25, 1959–1978. <https://doi.org/10.1016/j.csr.2005.07.001>.
- Nowell, A.R.M., Jumars, P.A., Eckman, J.E., 1981. Effects of biological activities on the entrainment of marine sediments. *Mar. Geol.* 42, 133–153.
- Safar, Z., 2022. *Suspended Particulate Matter Formation and Accumulation in the Delta: From Monitoring to Modelling*. PhD Thesis. Delft University of Technology.
- Shakeel, A., Safar, Z., Ibanez, M., Paassen, L., Chassagne, C., 2020. Flocculation of clay suspensions by anionic and cationic polyelectrolytes a systematic analysis. *Minerals* 1–24.
- Smith, S.J., Friedrichs, C.T., 2011. Size and settling velocities of cohesive flocs and suspended sediment aggregates in a trailing suction hopper dredge plume. *Cont. Shelf Res.* 31, S50–S63. <https://doi.org/10.1016/j.csr.2010.04.002>.
- Uncles, R.J., Stephens, J.A., Harris, C., 1998. Seasonal variability of subtidal and intertidal sediment distributions in a muddy, macrotidal estuary: the Humber-Ouse, UK. In: Black, K.S., Paterson, D.M., Cramp, A. (Eds.), *Sedimentary Processes in the Intertidal Zone*, vol. 139. Geological Society Special Publications, London, pp. 211–219.
- Van Leussen, W., 1999. The variability of settling velocities of suspended fine-grained sediment in the ems estuary. *J. Sea Res.* 41 (1), 109–118. [https://doi.org/10.1016/S1385-1101\(98\)00046-X](https://doi.org/10.1016/S1385-1101(98)00046-X).
- Whitehouse, R.J.S., Soulsby, R., Roberts, W., Mitchener, H.J., 2000. *Dynamics of Estuarine Muds*. Thomas Telford Publications, London.
- Winterwerp, J.C., 1998. A simple model for turbulence induced flocculation of cohesive sediment. *J. Hydraul. Res.* 36 (3), 309–326.